Neuron
Article

TRAK/Milton Motor-Adaptor Proteins Steer Mitochondrial Trafficking to Axons and Dendrites

Myrrhe van Spronsen,[1,3,7] Marina Mikhaylova,[1,5,7] Joanna Lipka,[1,6,7] Max A. Schlager,[3] Dave J. van den Heuvel,[2] Marijn Kuijpers,[1] Phebe S. Wulf,[1] Nanda Keijzer,[3] Jeroen Demmers,[4] Lukas C. Kapitein,[1] Dick Jaarsma,[3] Hans C. Gerritsen,[2] Anna Akhmanova,[1] and Casper C. Hoogenraad[1,3,*]
[1]Cell Biology, Department of Biology
[2]Molecular Biophysics, Department of Physics and Astronomy
Faculty of Science, Utrecht University, 3584 CH Utrecht, The Netherlands
[3]Department of Neuroscience
[4]Proteomics Center
Erasmus Medical Center, 3015 GE Rotterdam, The Netherlands
[5]RG Neuroplasticity, Leibniz-Institute for Neurobiology, 39118 Magdeburg, Germany
[6]International Institute of Molecular and Cell Biology, 02-109 Warsaw, Poland
[7]These authors contributed equally to this work
*Correspondence: c.hoogenraad@uu.nl
http://dx.doi.org/10.1016/j.neuron.2012.11.027

SUMMARY

In neurons, the distinct molecular composition of axons and dendrites is established through polarized targeting mechanisms, but it is currently unclear how nonpolarized cargoes, such as mitochondria, become uniformly distributed over these specialized neuronal compartments. Here, we show that TRAK family adaptor proteins, TRAK1 and TRAK2, which link mitochondria to microtubule-based motors, are required for axonal and dendritic mitochondrial motility and utilize different transport machineries to steer mitochondria into axons and dendrites. TRAK1 binds to both kinesin-1 and dynein/dynactin, is prominently localized in axons, and is needed for normal axon outgrowth, whereas TRAK2 predominantly interacts with dynein/dynactin, is more abundantly present in dendrites, and is required for dendritic development. These functional differences follow from their distinct conformations: TRAK2 preferentially adopts a head-to-tail interaction, which interferes with kinesin-1 binding and axonal transport. Our study demonstrates how the molecular interplay between bidirectional adaptor proteins and distinct microtubule-based motors drives polarized mitochondrial transport.

INTRODUCTION

Transport of mitochondria to meet local energy demands is critical in highly differentiated and polarized cells such as neurons. In the axon, mitochondrial ATP production supports the generation of action potentials and trafficking of synaptic vesicles, and in dendrites, it is needed for synaptic transmission. Mitochondria are concentrated in the cell body, which is often far away from the energy-demanding synapses. Thus, proper targeting of mitochondria from the cell body into dendrites and the axon is essential for the support of synapses and maintenance of axon and dendrites. Consistently, defective mitochondrial trafficking and function are increasingly implicated in neurological diseases (Chan, 2006; Mattson et al., 2008).

Several studies have shown that cytoskeletal motor proteins are responsible for transport of mitochondria in neurons (Boldogh and Pon, 2007; Frederick and Shaw, 2007; Saxton and Hollenbeck, 2012). In both axons and dendrites, the majority of these movements are microtubule based and characterized by alternating outward (or anterograde) and inward (or retrograde) transport, interspersed with periods of stationary docking (Kang et al., 2008; Pilling et al., 2006). Such bidirectional transport suggests that mitochondria interact with both families of microtubule-based motors, kinesins and dynein, which drive transport toward the microtubule plus end and minus end, respectively (Hirokawa and Noda, 2008; Vale, 2003). The regulatory mechanism of opposing motor activities is unknown but is of obvious importance to deliver mitochondria to the desired spatiotemporal locations (Saxton and Hollenbeck, 2012). These opposing motors are also involved in polarized transport and sorting of specific cargo between axons and dendrites (Kapitein and Hoogenraad, 2011; Rolls, 2011). In several model systems, it has been demonstrated that kinesin motors specifically target the axon and drive synaptic vesicle transport, whereas the dynein/dynactin motor complex sorts postsynaptic receptors and Golgi outposts to dendrites (Kapitein et al., 2010a; Zheng et al., 2008). While two different transport mechanisms exist to control polarized transport in neurons, it is unclear which machinery is used to uniformly distribute nonpolarized neuronal cargos, such as mitochondria.

Genetic screens in *Drosophila* for synaptic insufficiency have identified Mitochondrial Rho GTPase (Miro) (Guo et al., 2005) and trafficking protein, kinesin binding (TRAK)/Milton (Stowers et al., 2002) as being necessary for mitochondrial transport to

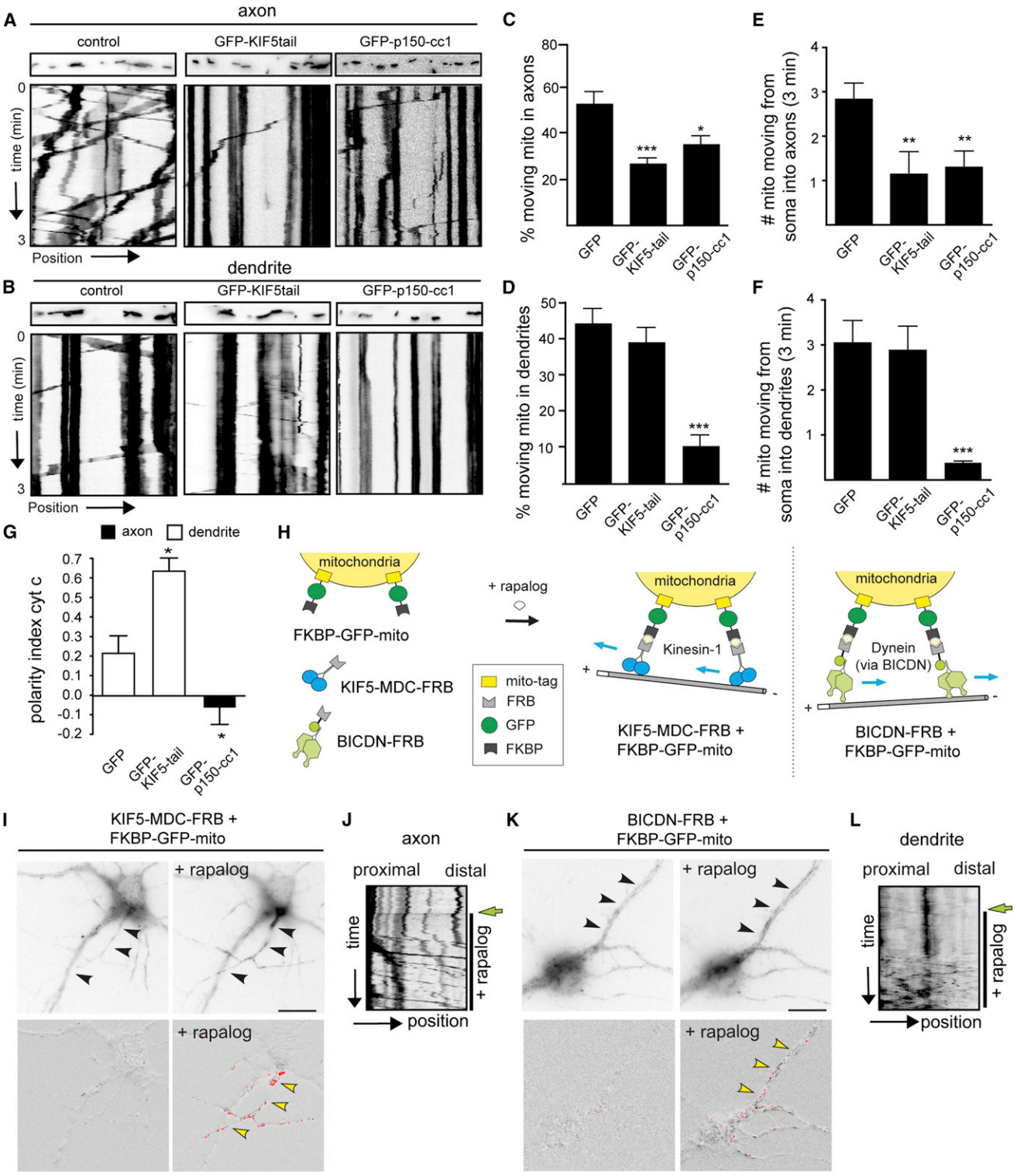

Figure 1. Kinesin-1 and Dynein Drive Polarized Mitochondria Transport in Neurons

(A and B) Hippocampal neurons were cotransfected with mito-dsRed and GFP (control), GFP-KIF5tail, or GFP-p150-cc1 (9 DIV for 4 days), and live-cell imaging microscopy was used to visualize mitochondrial motility in hippocampal neurons. Kymographs show the motility of mito-dsRed-labeled mitochondria in axons (A) and dendrites (B). Region of the kymographs in the representative axon or dendrite are indicated above.

(C–F) Quantification of mitochondrial transport in axons and dendrites includes percentage of the number of moving mitochondria (C and D) and number of mitochondria moving from the soma (E and F). Error bars indicate SEM (*$p < 0.05$, **$p < 0.01$, and ***$p < 0.001$).

(legend continued on next page)

synapses. Miro and TRAK are part of a conserved protein complex that is essential for mitochondrial distribution in neurons and many other cell types (Boldogh and Pon, 2007; Goldstein et al., 2008; MacAskill and Kittler, 2010). The TRAKs act as the motor-adaptor molecules that connect microtubules via kinesin-1/KIF5 to the mitochondria-anchored protein Miro. Recent studies showed that the Miro protein serves as a calcium sensor that regulates kinesin-mediated mitochondrial motility (Macaskill et al., 2009; Wang and Schwarz, 2009). Whereas *Drosophila* carries one TRAK/Milton gene, mammals have two different TRAK/Milton orthologs, named TRAK1 and TRAK2 (i.e., Milton-1/OIP106 and Milton-2/GRIF-1, respectively) (Brickley et al., 2005). All TRAK/Milton family proteins consist of an N-terminal coiled-coil region with homology to the huntingtin-associated protein 1 (HAP1) domain, found in several kinesin and dynein-interacting proteins, and the C-terminal domain of TRAK/Milton interacts with Miro (Glater et al., 2006; Stowers et al., 2002). The high degree of similarity between the mammalian TRAK family members of proteins suggests that they may have redundant functions; however, this has not previously been investigated.

Here, we use a large variety of immunohistochemical, biochemical, cell biological, live-cell imaging, and quantitative microscopy approaches to demonstrate that TRAK1 and TRAK2 differentially regulate polarized sorting of mitochondria. Our data show that TRAK1 binds to both kinesin-1/KIF5B and dynein/dynactin and steers mitochondria into axons, whereas TRAK2 predominantly interacts with dynein/dynactin and mediates dendritic targeting. Depletion of TRAK1 reduces axon outgrowth and branching, whereas TRAK2 knockdown displays similar defects in dendrites. The difference between the two TRAK proteins arises from TRAK2's preference for a folded conformation, which is inhibitory for the binding to KIF5B and, hence, for axonal transport. We propose a model in which kinesin-1 drives mitochondria transport into axons and requires dynein for its activity (controlled by TRAK1), and dynein steers mitochondria trafficking into dendrites independently of kinesin-1 (controlled by TRAK2). Our findings advance the knowledge of fundamental transport processes essential for the maintenance of neuronal homeostasis and have important implications for our understanding of neuronal degeneration.

RESULTS

Polarized Sorting of Mitochondria Is Regulated by Kinesin-1 and Dynein Motor Proteins

Mitochondria hold different types of motor proteins, and their opposing activity most likely leads to bidirectional transport in both axons and dendrites. Recent data demonstrated that opposing motors are not only required to drive bidirectional motion but also play an important role in controlling polarized cargo transport into axon and dendritic processes (Kapitein and Hoogenraad, 2011; Rolls, 2011). To test whether kinesin-1 and dynein motor activity are required for proper targeting of mitochondria to axons and dendrites, we used live-cell video microscopy to visualize mitochondrial motility in hippocampal neurons (Movie S1 available online) that were transfected with GFP-tagged dominant-negative kinesin-1 construct (KIF5-tail) or the dominant-negative dynactin construct (p150-cc1). Mitochondria transport parameters in both axons and dendrites were analyzed using kymographs and tracking software. Expression of GFP-KIF5-tail in hippocampal neurons results in a strong reduction of moving mitochondria in the axon, while motility in dendrites is normal compared to control (Figures 1A and 1C; Movie S2). In contrast, expression of GFP-p150-cc1 decreased the number of moving mitochondria in both axons and dendrites (Figures 1A–1D; Movies S2 and S3). In all cases, the reduced motility is observed in both retrograde and anterograde directions in axons and dendrites (Table S1). To specifically test whether these manipulations can disrupt axonal and dendritic targeting, we analyzed the number of mitochondria from the soma that enter these compartments. Axonal targeting is strongly reduced by blocking KIF5 or dynein/dynactin, while dendritic entry is only affected by inhibiting dynein/dynactin activity (Figures 1E and 1F). Analyzing the velocity and run length of the residual mitochondrial movements in GFP-KIF5-tail and GFP-p150-cc1-expressing neurons revealed no marked changes in these dynamic parameters (Figure S1; Table S1). These results demonstrate that kinesin-1 and dynein strongly affect the frequency of mitochondria movement, but not the speed and run length. Moreover, kinesin-1 and dynein cooperate to control axonal movement, while dendritic motility requires dynein, but not kinesin-1.

Next, we tested the effect of these manipulations on mitochondria distributions in hippocampal neurons. The distribution of endogenous mitochondria, as revealed by mitochondria marker cytochrome *c*, in GFP-KIF5-tail and GFP-p150-cc1-expressing neurons was dramatically different from controls. Blocking kinesin-1 redistributed mitochondria away from the axon into the dendrites, while inhibition of dynein led to a few more mitochondria in axons. To quantify the mitochondria dendrite-to-axon ratio, we measured the average dendrite intensity (Id) and average axonal intensity (Ia) and calculated the polarity index (PI) by using $PI = (Id-Ia)/(Id+Ia)$ (Kapitein et al., 2010a). For uniformly distributed proteins, Id = Ia and PI = 0, whereas $PI > 0$ or $PI < 0$ indicates polarization toward dendrites and axons, respectively. Analysis of cytochrome *c* in control neurons for the mitochondria distribution yielded a PI of

(G) PI of cytochrome *c* (cyt c) intensity in GFP (control), GFP-KIF5-tail, and GFP-p150-cc1-transfected neurons (12 DIV for 2 days) as indicated. Error bars indicate SEM. *$p < 0.05$.

(H) Inducible mitochondria-trafficking assay. Fusions of FRB with the truncated motor construct of kinesin-1 (KIF5-MDC-FRB) and dynein adaptor Bicaudal D2 (BICDN-FRB) are recruited to FKBP-GFP-mito upon addition of rapalog.

(I and K) Representative images of hippocampal neurons at 15 DIV coexpressing FKBP-GFP-mito and KIF5-MDC-FRB (I) and BICDN-FRB (K) before and after addition of rapalog. Black arrowheads indicate mitochondria in axons and dendrites. The differential translocation of mitochondria (pseudocolor red) before and after rapalog treatment is indicated (yellow arrowheads). Scale bars, 20 μm.

(J and L) Kymograph of mitochondria movement in axons (J) and dendrites (L) from recordings shown in (I) and (K). Green arrows indicates the addition of rapalog. See also Figures S1 and S2, Movies S1, S2, S3, S4, and S5, and Table S1.

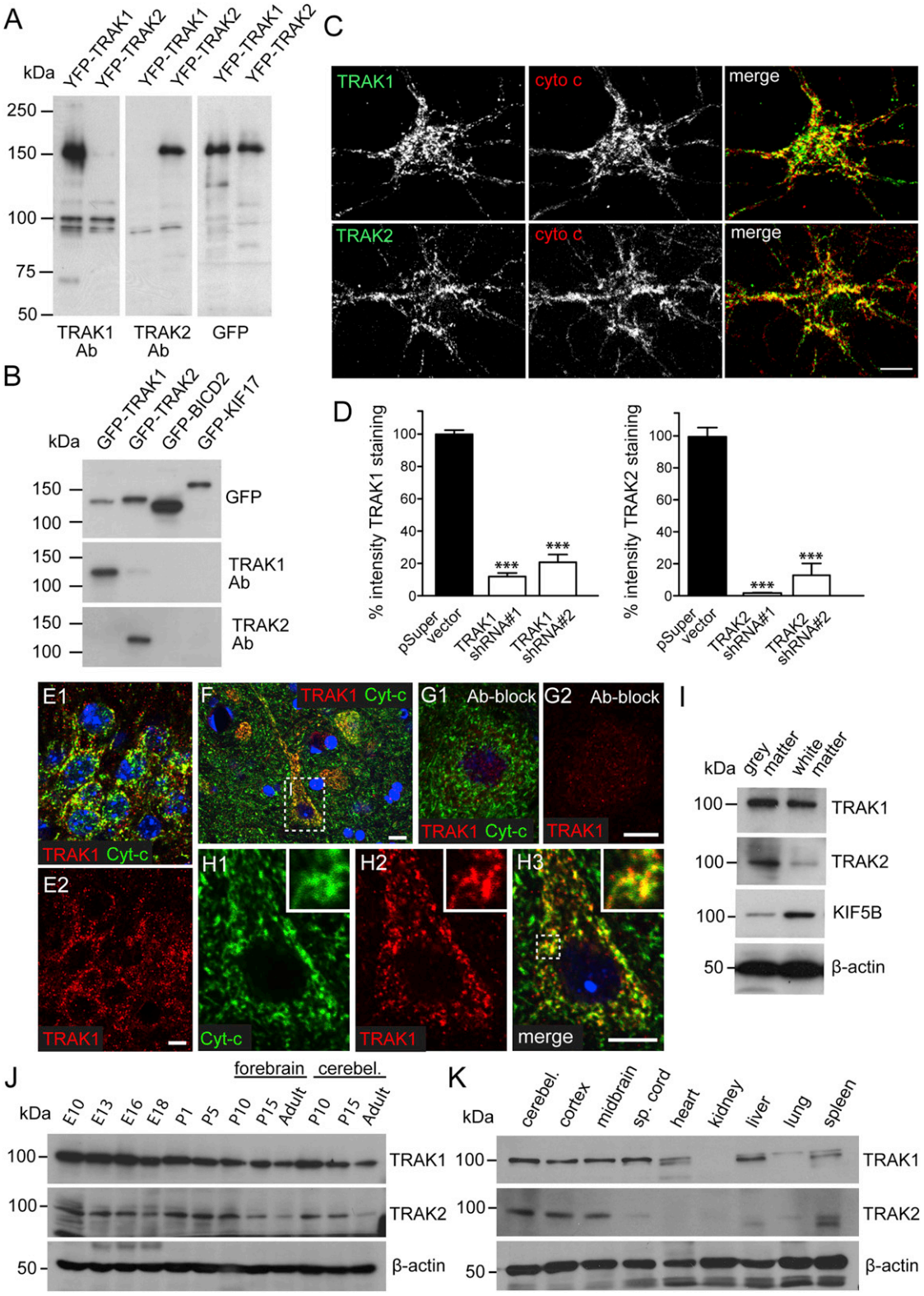

Figure 2. TRAK Proteins Are Differentially Distributed in the CNS

(A) Specificity of anti-TRAK antibodies. Lysates from HEK293 cells transfected with YFP-TRAK1 and YFP-TRAK2 analyzed by western blotting with anti-GFP, anti-TRAK1, or anti-TRAK2 antibodies. YFP refers to the YFP-TRAK-CFP constructs, which runs at ~150 kDa on immunoblots and allows better separation with endogenous TRAK proteins (~100 kDa).

(legend continued on next page)

0.22 ± 0.09 (Figure 1G), demonstrating that there are slightly more mitochondria present in dendrites compared to the axon. Blocking kinesin-1 reveals a positive PI of 0.62 ± 0.09 (more abundant in dendrites), while inhibition of dynein shows a PI of −0.05 ± 0.14 (more in the axon) (Figure 1G), indicating that kinesin-1 and dynein are necessary for the proper polarized distribution of mitochondria in axons and dendrites.

Kinesin-1 and Dynein Establish Axon and Dendrite-Specific Targeting

To directly address whether recruitment of kinesin-1 and dynein motor activity to mitochondria is sufficient to establish axon and dendrite-specific targeting, we made use of an inducible mitochondria-trafficking assay (Hoogenraad et al., 2003; Kapitein et al., 2010b). In this assay, FRB-FKBP heterodimerization is used in combination with the cell-permeable rapamycin analog AP21967 (from now on called rapalog) to trigger the binding of the motor proteins of interest to mitochondria. Mitochondria were labeled by expressing FKBP-GFP-mito, a fusion construct of the Listeria ActA mitochondria-targeting sequence (mito) to green fluorescent protein (GFP), and FKBP12, a domain that can be crosslinked to FRB in the presence of rapalog (Hoogenraad et al., 2003) (Figure 1H). FRB is fused to truncated kinesin-1, which contains the motor domain and coiled-coil dimerization region (KIF5-MDC-FRB) and the N-terminal part of the dynein/dynactin accessory protein Bicaudal-D (BICDN-FRB) (Hoogenraad et al., 2003; Kapitein et al., 2010b) (Figure 1H). Addition of rapalog to neurons coexpressing KIF5-MDC-FRB and FKBP-GFP-mito induced a rapid burst of mitochondria from the cell body into the axon (Figure 1I; Movie S4). Acquisition of zoomed regions at increased frame rates (5 frames/s) revealed that the majority of mitochondria in axons after rapalog addition moved in anterograde direction (from proximal to distal; Figures 1J, S2A, and S2C). No mitochondria movement was observed in dendrites after KIF5-MDC-FRB recruitment (Figures S2A and S2C). In contrast, addition of rapalog to neurons expressing BICDN-FRB caused mitochondria to move away from the cell body into the primary dendrites (Figure 1K; Movie S5). We observed that mitochondria coupled to dynein target the dendrites with bidirectional runs (Figures 1L, S2B, and S2D), which is consistent with dynein-coupled cargos moving into dendrites along antiparallel microtubules (Kapitein et al., 2010b). Addition of rapalog to these neurons also drives retrograde transport of mitochondria already present in axons (Figures S2B and S2D). Altogether, these data demonstrate that the opposing kinesin-1 and dynein motor proteins are both necessary and sufficient for the proper distribution of mitochondria to axons and dendrites, respectively.

Differential Distribution of TRAK Proteins in the CNS

We hypothesized that regulatory motor-adaptor proteins might exist that steer mitochondria transport into axons and dendrites. We focused on the TRAK family because these adaptor proteins were previously found to associate with kinesin-1 and regulate mitochondrial transport in neurons (Macaskill et al., 2009; Wang and Schwarz, 2009). To study the roles of mammalian TRAK family members in neuronal mitochondrial trafficking, we first generated rabbit polyclonal antibodies to TRAK1 and TRAK2 proteins. Both newly generated antibodies reacted strongly and specifically with the appropriate TRAK protein on western blot and did not recognize the other TRAK ortholog or control proteins (Figures 2A and 2B). Antibody specificity was also demonstrated by immunofluorescence stainings in GFP-TRAK1/TRAK2-transfected HeLa cells (data not shown). The TRAK1 and TRAK2 antibodies showed more than ~80% reduction of punctuate-staining intensity in TRAK1 or TRAK2-shRNA-expressing primary hippocampal neurons, respectively, at 14 days in vitro (DIV14) (Figures 2C, 2D, and S3). Moreover, the punctate staining in various neuronal cell types in the CNS, including pyramidal neurons in the hippocampus (Figure 2E), was blocked by preincubating the antibodies with the corresponding TRAK antigens (Figure 2G; data not shown). The ability of both TRAK proteins to associate with mitochondria was confirmed by the colocalization of endogenous TRAK proteins and cytochrome *c* (Figure 2C) in mouse brain and spinal cord sections (Figures 2E–2H). We found ~80% (TRAK1) and ~70% (TRAK2) overlap with the mitochondrial marker cytochrome *c*.

In agreement with in situ hybridization data from the Allen Mouse Brain Atlas and the immunohistochemical experiments (Figures 2E–2H), western blot analysis of various adult mouse tissues showed that both TRAK1 and TRAK2 are expressed throughout the developing and adult brain (Figure 2J). TRAK2 is predominantly expressed in cerebellum, cortex, and midbrain, whereas TRAK1 is also detected in several other organs outside the brain, including heart, liver, lung, and spleen (Figure 2K). Within the regions of the murine nervous system examined, TRAK1 and TRAK2 expression varied mostly in the spinal cord (Figure 2K). In this axon-rich tissue, TRAK1 protein is readily

(B) Protein extracts of HeLa cells transfected with GFP-TRAK1, GFP-TRAK2, and two negative control constructs (GFP-BICD2 and GFP-KIF17) were analyzed by western blotting with anti-GFP, anti-TRAK1, or anti-TRAK2 antibodies.
(C) Representative images of hippocampal neurons at DIV14 stained for endogenous TRAK1 or TRAK2 (green) and mitochondria marker cytochrome *c* (red). Scale bar, 10 μm.
(D) Quantification of TRAK1 and TRAK2 fluorescent-staining intensities in cell body of hippocampal neurons transfected at DIV12 for 4 days with GFP and TRAK-shRNAs. The staining is normalized to the nontransfected surrounding cells in the same image. ***$p < 0.001$.
(E–H) Triple labeling of TRAK1 (red), cytochrome *c* (green), and DAPI (blue) in CA3 of hippocampus of adult mouse (E) and motor neurons of the mouse spinal cord (F–H). The square in (F) corresponds to (H1–H3). TRAK1 antibody is blocked with its own antigen in (G). The inset in (H) is an enlarged region of the cell, as indicated by the dotted square in (H3). Scale bars, 100 μm.
(I) Western blots of TRAK and KIF5B expression in extracts from cortex (gray matter) and spinal cord (white matter) of rat.
(J) Developmental expression patterns of TRAK1 and TRAK2 in E10.5 (whole embryo), E13, E16, E18, and P1, P5 (head only), and P10, P15, and adult (forebrain or cerebellum) mouse.
(K) Western blot analysis of TRAK1 and TRAK2 in various adult mouse tissues, including brain regions and organs. cerebel., cerebellum; sp. cord, spinal cord. See also Figure S3.

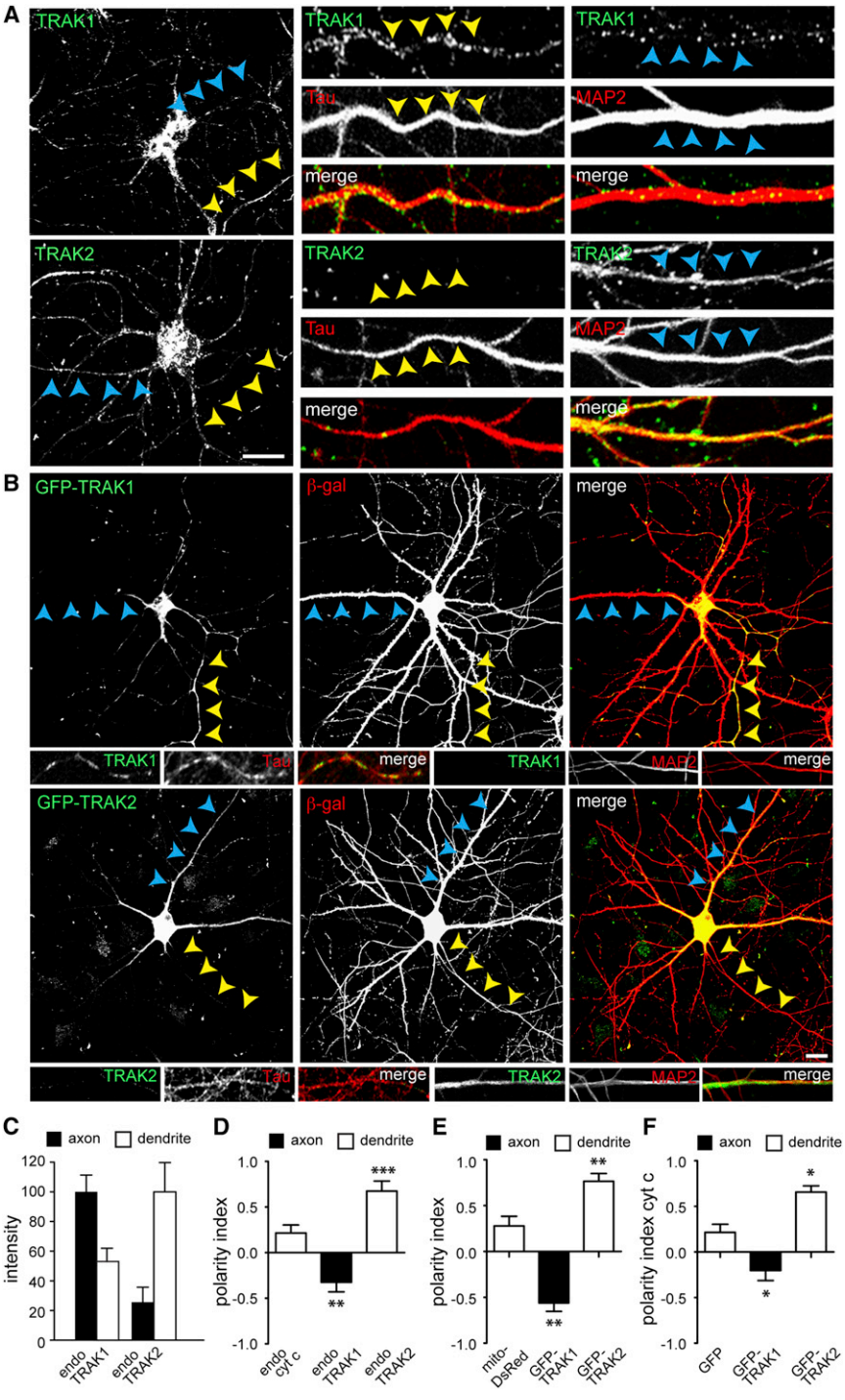

Figure 3. Polarized Distribution of TRAK Proteins in Hippocampal Neurons

(A) Representative images of hippocampal neurons (DIV 14) stained for endogenous TRAK1 and TRAK2 (green) and costained with Tau and MAP2 (red) to highlight axon and dendrites. Yellow arrowheads indicate axons, and blue arrowheads indicate dendrites. Scale bar, 20 μm.

(B) Representative images of hippocampal neurons (DIV 12+2) cotransfected with GFP-TRAK1 or GFP-TRAK2 and β-gal to visualize neuronal morphology. Yellow arrowheads indicate axons, and blue arrowheads indicate dendrites. Scale bar, 20 μm.

(C) Quantification of endogenous TRAK1 and TRAK2 intensity in axons and dendrites of hippocampal neurons at DIV 14. Normalized intensity is the highest fluorescent intensity in axons or dendrites and set at 100.

(D) PI of endogenous cytochrome *c* (as control), TRAK1, and TRAK2 in hippocampal neurons at DIV 14.

(E) PI of exogenous mitochondria marker mito-dsRed, GFP-TRAK1, and GFP-TRAK2 in hippocampal neurons at DIV 12+ 2.

(F) PI of endogenous cytochrome *c* intensity in GFP (as control), GFP-TRAK1, and GFP-TRAK2-transfected neurons (DIV 12+2).

Error bars indicate SEM. $^{*}p < 0.05$, $^{**}p < 0.01$, and $^{***}p < 0.001$.

See also Figure S4.

detected, whereas TRAK2 protein is barely present, an observation confirmed by comparing the expression of the two TRAK proteins in cerebral gray and cervical spinal white matter (Figure 2I). The low expression of TRAK2 in the spinal cord is unexpected for a protein predicted to be involved in axonal transport. In fact, the axonal transport motor KIF5B is present at higher levels in the white matter in spinal cord compared to the cortex (Figure 2I). Together, these data show that both TRAK1 and TRAK2 associate with mitochondria but have a differential distribution in the CNS.

Polarized Distribution of TRAK Proteins in Hippocampal Neurons

We next tested whether TRAK1 and TRAK2 proteins are differentially distributed in cultured hippocampal neurons. Although both TRAK1 and TRAK2 antibodies label the neuronal cell body, axon, and dendrites (Figure 2C), the localization patterns in axons and dendrites are markedly different from each other. Double-labeling immunofluorescence experiments for each TRAK protein and the axonal marker Tau or the dendritic marker MAP2 revealed a more prominent localization of TRAK1 in axons and TRAK2 in dendrites (Figure 3A). To further quantify the differential TRAK1 and TRAK2 distribution in neurons, we measured the average intensity in axon and dendrites (Figure 3C) and calculated the PI. Quantification of the intensity of TRAK1 antibody staining reveals a negative PI of −0.32 ± 0.11 (more abundant in axons), while TRAK2 has a positive PI of 0.68 ± 0.11 (more abundant in dendrites) (Figure 3D), indicating a polarized distribution of endogenous TRAK proteins in hippocampal neurons. The opposing distribution of the two TRAK proteins was even more

apparent by expression of fluorescently tagged TRAK1 and TRAK2: GFP-TRAK1 mainly targeted the axons, while GFP-TRAK2 was almost exclusively present in dendrites (Figures 3B and 3E). Interestingly, GFP-TRAK2 is mainly localized to primary dendrites but is less prominent in higher-order branches. Next, we investigated whether the expression of TRAK proteins can influence the normal mitochondrial distribution in neurons. Neurons transfected with GFP-TRAK1 or GFP-TRAK2 dramatically shifted the mitochondrial localization to axons or dendrites, respectively (Figure 3F). The opposing effects on mitochondria localization were also observed in cultured HeLa cells: expression of GFP-TRAK1 induced formation of peripheral mitochondrial clusters, while GFP-TRAK2 caused strong accumulation of mitochondria in the cell center (Figure S4). Together, these data show that TRAK1 and TRAK2 have differential effects on mitochondria distribution: TRAK1 is prominently localized in axons, while TRAK2 is more abundantly present in dendrites.

TRAK Proteins Control Mitochondrial Motility in Axons and Dendrites

Recent data suggest that TRAK1 is required for mitochondrial transport within axons of hippocampal neurons (Brickley and Stephenson, 2011). To further explore the function of TRAK proteins in mitochondrial motility, we used live-cell video microscopy and observed that knockdown of TRAK1/TRAK2 disrupts mitochondrial motility in both axons and dendrites (Figures 4A–4D; Movies S6 and S7). In the absence of both TRAK proteins, mitochondrial motility was reduced by ~65% in axons and by ~45% in dendrites (Figures 4C and 4D). Interestingly, expression of TRAK1-shRNA in neurons results in a strong reduction of moving mitochondria in axons compared to control cells (Figure 4C). In contrast, expression of TRAK2-shRNA does not affect motility in axons but decreases the number of moving mitochondria in dendrites (Figures 4C and 4D). In all cases, the reduced motility is observed in both retrograde and anterograde directions in axons and dendrites (Table S1). Further characterization of the residual mitochondria dynamics in TRAK knockdown neurons showed no marked changes in velocity and run length (Figure S1; Table S1), similar to kinesin-1 and dynein/dynactin inhibition. Together, these results indicate that TRAK proteins are important for mitochondrial transport in axons and dendrites: TRAK1 is required for proper axonal trafficking of mitochondria, whereas TRAK2 is needed for dendritic mitochondria motility.

TRAK Proteins Are Required for Normal Morphology of Axons and Dendrites

Given previous observations that dysfunction and defective transport of mitochondria alter neuronal morphology (Chan, 2006), we examined the effect of TRAK1/TRAK2 knockdown on the outgrowth of axons and dendrites. In developing neurons coexpressing TRAK1 and TRAK2 shRNAs and β-galactosidase (β-gal; to highlight neuronal morphology), we observed a marked change in morphology of both axons and dendrites (Figure 4E). Quantification revealed that the length of axons and dendrites was decreased by ~50% in TRAK1/TRAK2 double-knockdown cells compared to control neurons (Figures 4F–4K). A similar morphological phenotype was observed after expressing dominant-negative forms of TRAK1 and TRAK2 (Figure S5), which contains only the C-terminal Miro-binding domain and inhibits the binding of endogenous TRAK1/TRAK2 to mitochondria. We next analyzed single TRAK1 and TRAK2 depletions and observed that axon morphology of neurons expressing TRAK1-shRNA was severely affected, while neurons expressing TRAK2-shRNA showed a marked decrease in dendritic outgrowth (Figure 4E). Quantification indicated that knockdown of TRAK1 decreases axon length, the number of axonal tips, and the number of axonal branches by ~50%, compared to control neurons (Figures 4F–4H). In contrast, knockdown of TRAK2 decreased total dendritic length and number of primary dendrites by ~50%, while the cell soma size was not significantly changed (Figures 4I–4K). The second set of independent TRAK1 and TRAK2 shRNAs gave similar phenotypes (data not shown). Together, these results indicate that TRAK proteins are required for normal neuronal morphology: TRAK1 plays an essential role in axonal outgrowth, while TRAK2 is critically important for dendrite morphology.

Differential Interaction of TRAK1 and TRAK2 with Kinesin-1 and Dynein

To better understand the differential role of TRAK proteins in mitochondria transport, we next searched for distinct TRAK1 and TRAK2-binding partners. Biotinylated and GFP-tagged TRAK1 and TRAK2 (bio-GFP-TRAK1 and bio-GFP-TRAK2) and bio-GFP as a control construct were transiently coexpressed in HEK293 cells together with the protein-biotin ligase BirA, isolated with streptavidin beads, incubated with rat brain extracts, and isolated proteins were analyzed by mass spectrometry. Both bio-GFP-TRAK1 and bio-GFP-TRAK2 bound to the previously identified TRAK partners, including atypical GTPase Miro (Miro1 or Miro2) (Glater et al., 2006) and O-linked N-acetylglucosamine (O-GlcNAc) transferase (OGT) (Iyer et al., 2003) (Figure 5A; Table S2). In addition, potential TRAK-binding partners were identified, such as several components of dynein and dynactin complexes, including dynein heavy-chain 1 (DHC1), dynein light-chain 1 (DLC1), p150Glued, and p50/dynamitin (Figure 5A). These mass spectrometry results were confirmed by western blotting (Figure 5B) and immunoprecipitation experiments with GFP-p150Glued (Figure 5C), indicating that both TRAK1 and TRAK2 bind to the dynein/dynactin motor complex. To get further insights into the structural features determining the dynein/dynactin binding to TRAK, we explored whether TRAK can interact with one distinct subunit in the dynein/dynactin complex. TRAK1 or TRAK2 was coexpressed with cytoplasmic dynein and dynactin subunits, and interactions were assessed by pull-down assays. Both TRAK proteins were precipitated with the p150Glued subunit of dynactin (Figure 5F), while the N-terminal tail domain of DHC or the DIC and DLIC subunits of the dynein complex were negative in this assay. Expression of GFP-TRAK1 or GFP-TRAK2 revealed colocalization with dynein/dynactin in HeLa cells, especially in the pericentral region (Figure 5G; data not shown) and in the cell body of hippocampal neurons (data not shown). These results indicate that both TRAK proteins interact with the p150Glued subunit of the dynactin complex.

Next, we screened the mass spectrometry data for proteins that showed specific affinity for either TRAK1 or TRAK2 and

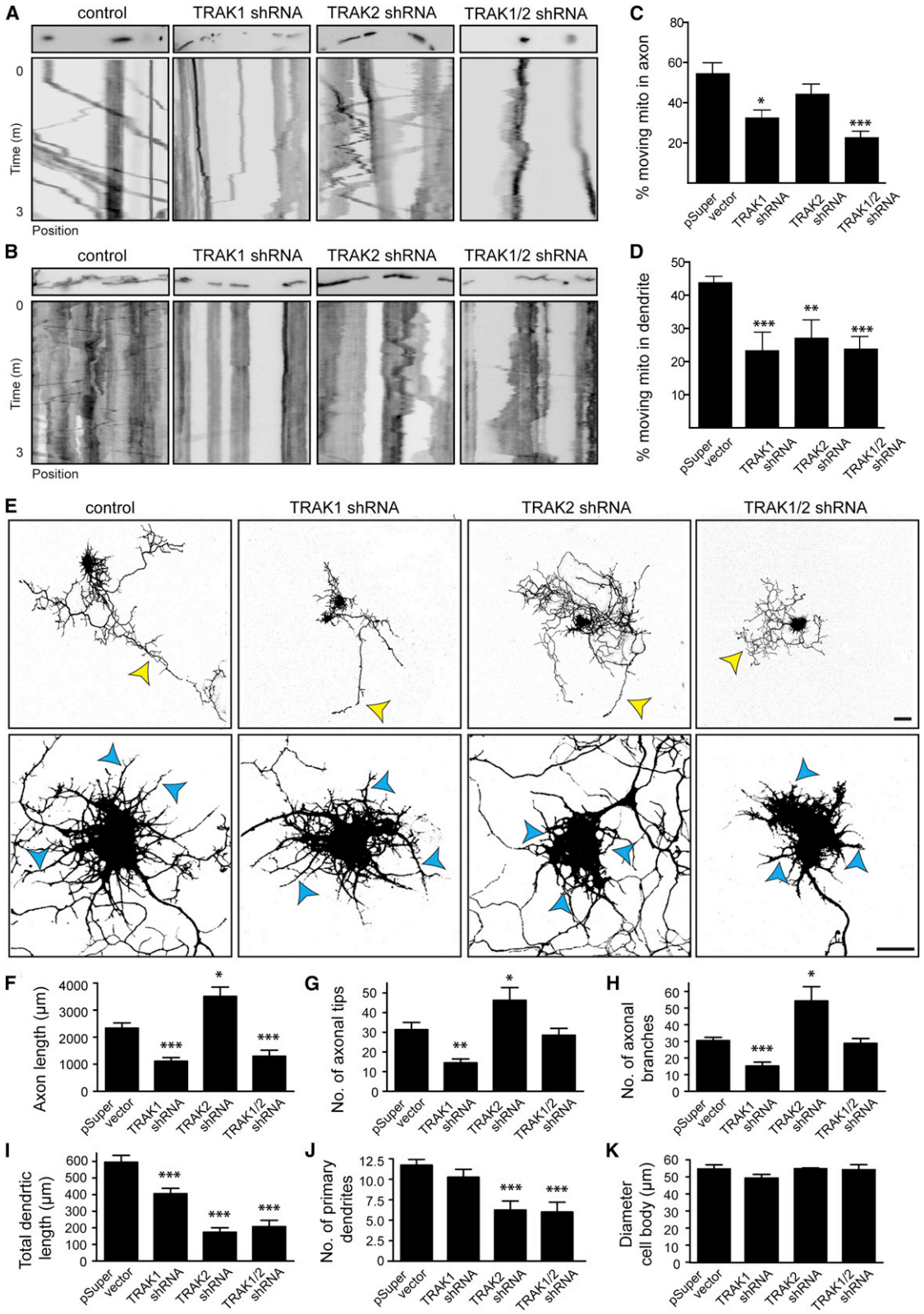

Figure 4. TRAK Proteins Are Required for Mitochondrial Motility and Axon and Dendrite Morphology

(A and B) Kymographs show the motility of mitochondria, labeled with mito-dsRed in axons (A) and dendrites (B). Hippocampal neurons were cotransfected with mito-dsRed and indicated shRNA constructs. Regions of the kymographs in the representative axon or dendrite are indicated.

(legend continued on next page)

found that KIF5B was highly enriched in the TRAK1 biotin pull-down compared to the TRAK2 pull-down (26 versus 2 unique KIF5B peptides) (Figure 5A; Table S2). Additional biotin pull-down and mass spectrometry experiments from other cell lines also detected a strong enrichment of KIF5B peptides in the TRAK1 sample (Figure 5B; data not shown). Indeed, endogenous KIF5B showed higher binding to TRAK1 in coimmunoprecipitation experiments compared to TRAK2, while Miro associated with both TRAK proteins (Figure 5D). When KIF5B was overexpressed, it bound equally well to TRAK1 and TRAK2 (Figures 5E and 5F), suggesting that TRAK2 does not associate with endogenous kinesin-1 motors, but overexpression can induce the interaction between TRAK2 and KIF5B. Consistent with previous data from Glater et al. (2006), we did not find kinesin light chain (KLC), a major binding partner of kinesin-1, in the TRAK1 pull-down (Figures 5A and 5B), indicating that the association between TRAK1 and KIF5 does not require KLC. Together, these data show that TRAK adaptors associate with a distinct composition of motor complexes; both TRAKs bind to the dynactin subunit p150Glued, and only TRAK1 shows a strong interaction with kinesin-1.

Mapping the Binding Region between TRAK1, KIF5B, and p150Glued

To get further insights into the kinesin-1 and dynein/dynactin binding to TRAK proteins, we mapped the regions of TRAK1 responsible for KIF5B and p150Glued binding. The NH2 terminus of TRAK1 (amino acids 1–395, TRAK1-N) contains two predicted coiled-coil domains (Figures S6A and S6B), with the first one covering amino acids 100–200 and the second one from 201 to 360. Based on these N-terminal coiled-coil regions, we produced a series of TRAK1 deletion mutant constructs (Figure S6C). Full-length GFP-KIF5B or full-length GFP-p150Glued was coexpressed with different TRAK1 deletion fragments fused to bio-mCherry in HEK293 cells and immunoprecipitated using GFP-trap magnetic beads. As expected (Glater et al., 2006), GFP-KIF5B was coimmunoprecipitated with TRAK1-N and not TRAK1-C (Figures S6C and S6D). Truncating TRAK1-N showed that TRAK1_1–360 and TRAK1_101–360 were still efficiently binding to KIF5B, and the shortest binding region could be reduced down to the second coiled-coil region, amino acids 201–360 (Figures S6C and S6D). Further shortening of this region completely abolished binding of KIF5B (data not shown). The p150Glued interaction required the complete N-terminal domain (amino acids 1–360) of TRAK1 (Figures S6C and S6E). Interestingly, GFP-p150Glued was also found to bind to the C-terminal domain of TRAK1 (TRAK1-C). These data demonstrate that TRAK proteins contain one N-terminal KIF5B-binding region and two dynein/dynactin-binding sites, one at the N-terminal and one at the C-terminal domain.

The TRAK N-Terminal Domain Mediates Both KIF5B and Dynein-Dependent Motility

To more directly study the functional interaction between TRAK proteins and kinesin-1 and dynein/dynactin motors, we again turned to the inducible cargo-trafficking assay but now used peroxisomes as a tool to report the cargo transport activity of TRAK proteins (Kapitein et al., 2010b). Peroxisomes were labeled by expressing PEX-RFP-FKBP, a fusion construct of PEX3 peroxisomal membrane-targeting signal to the red fluorescent protein (RFP), and FKBP12 (Figure 6A). Since the N-terminal domain of TRAK binds to both kinesin-1 and dynein/dynactin (Figure 5), we generated constructs where FRB was fused to TRAK1-N and TRAK2-N (TRAK1-N-FRB and TRAK2-N-FRB) to determine whether the N-terminal TRAK fragments can induce microtubule plus-end and/or minus-end-directed movements. In COS7 cells transfected with PEX-RFP-FKBP and any of the two TRAK-N-FRB constructs, most peroxisomes were randomly distributed, while treating these cells with rapalog revealed a robust clustering in the cell periphery. Quantification of the peroxisomal distribution indicated that ~40% of the TRAK1-N-FRB and TRAK2-N-FRB cells showed peripheral peroxisome clusters, compared to non in control cells (Figures 6I and 6J). Next, we performed live-cell imaging experiments and confirmed the directional translocation of peroxisomes to the cell periphery, similar to KIF5-driven peroxisome motility but also observed a redistribution of some peroxisomes to more central regions of the cell, similar to dynein-driven peroxisome movement (Figure 6B; Movie S8). The average speed and displacement of the TRAK-N-coupled peroxisomes are markedly lower when compared to KIF5-MDC-FRB (Figures 6C–6E). Interestingly, fast acquisition (1 frame/s) to probe motility of individual peroxisomes revealed that these cargos could move bidirectionally when attached to TRAK1-N-FRB or TRAK2-N-FRB (Figures 6F–6H). Given that in cells with a radial microtubule array such as COS7, bidirectional movement is only observed when peroxisomes are coupled to both kinesin and dynein motors (Kapitein et al., 2010b), the data suggest that the N-terminal domain of TRAK mediates both kinesin-1 and dynein/dynactin-dependent motility.

To further test this, we explored the effect of KIF5B knockdown and inhibition of dynein/dynactin by HA-p50/dynamitin on TRAK-N-mediated peroxisomal transport. While in ~40%, control cells expressing TRAK1-N-FRB or TRAK2-N-FRB peripheral peroxisome clusters were present after rapalog treatment, the peroxisomes shifted to the perinuclear region in ~90% of KIF5B-depleted cells (Figure 6J). A similar distribution was seen when peroxisomes were linked to the DHC-MDC-FRB (Figure 6B), suggesting that, in the absence of KIF5B, the minus-end-directed dynein motor complex actively transports TRAK-N-coupled peroxisomes. Indeed, the tight accumulation

(C and D) Percentage of the number of moving mitochondria in axons (C) and dendrites (D) of control and shRNA-transfected neurons as indicated and calculated from different imaging recordings.
(E) Representative images of hippocampal neurons cotransfected at DIV 1+4 with indicated shRNA constructs and GFP to visualize the neuron morphology. Yellow arrowheads indicate axons, and blue arrowheads highlight some typical dendrites. Scale bar, 20 μm.
(F–K) Quantification of axon and dendrite morphological parameters of hippocampal neurons, including axonal length (F), number of axonal tips (G), number of axonal branches (H), total dendrite length (I), number of primary dendrites (J), and diameter of cell body (K).
Error bars indicate SEM. *$p < 0.05$, **$p < 0.01$, and ***$p < 0.001$.
See also Figure S5 and Movies S6 and S7.

A

Identified proteins	protein acc./id	Molecular weight (Da)	Mascot Score TRAK1	Mascot Score TRAK2	Unique peptides TRAK1	Unique peptides TRAK2
OGT	gi|31873825	118088	2406	1958	31	32
Miro1	gi|119600651	53899	128	57	2	2
Miro2	gi|25187967	69067	81	167	2	4
KIF5B	gi|4758648	110358	2004	97	26	2
Dynein HC1	gi|33350932	534809	513	260	23	25
Dynein LC1	gi|83267866	10530	729	368	4	4
p150Glued	gi|13259510	142348	156	83	6	3
p50/dynamitin	gi|5453629	44906	28	58	1	2

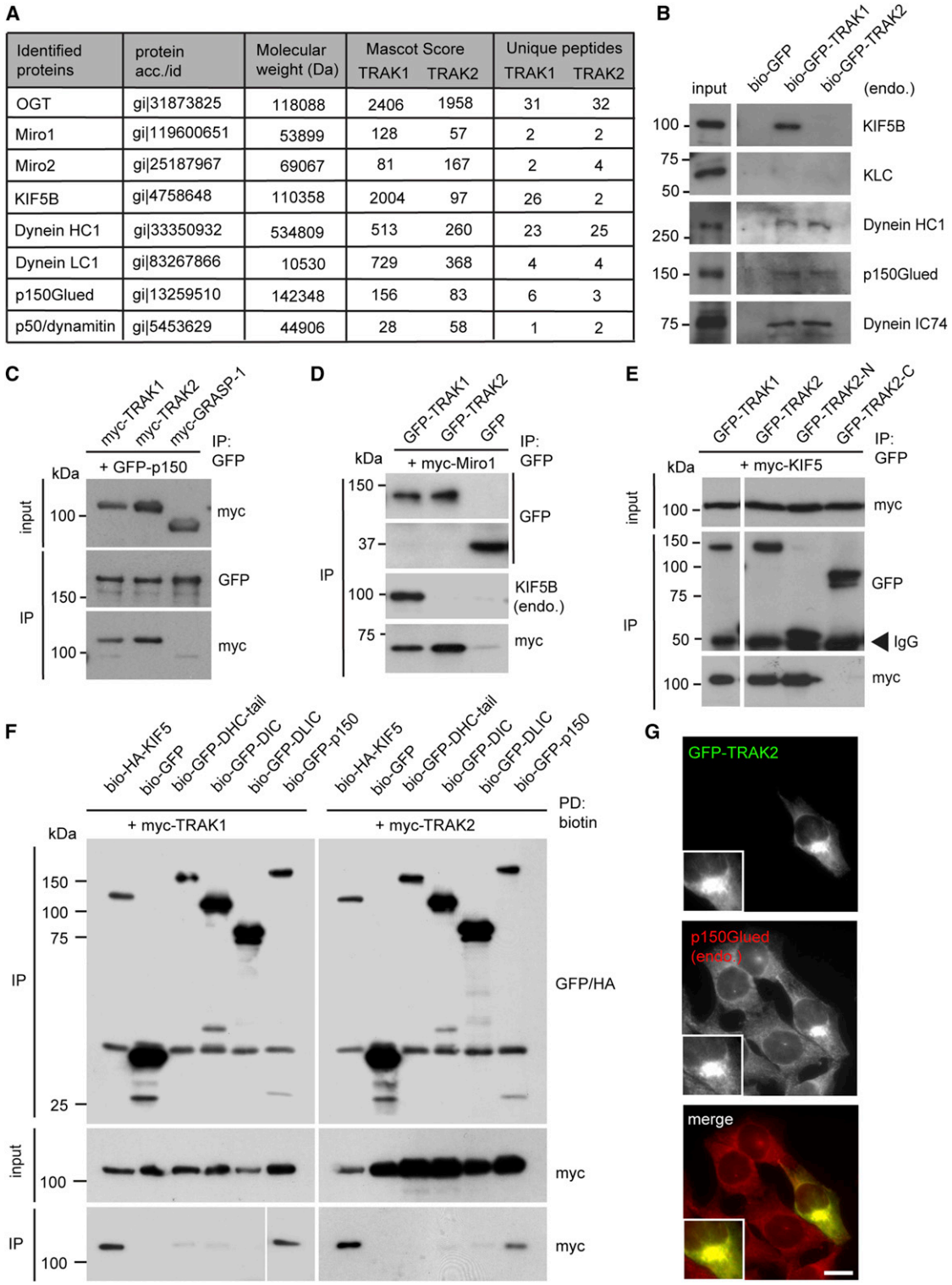

Figure 5. TRAK Proteins Bind to Dynein/Dynactin and Differentially to KIF5B

(A) Binding partners of bio-GFP-TRAK in HEK293 cells loaded with brain extracts and identified by mass spectrometry. acc./Id, accession number/identification number.

(B) Verification of interactions between TRAK1 or TRAK2 and their endogenous (endo.) binding partners identified by mass spectrometry using biotin pull-down assay and subsequent western blot analysis. Equal volumes of total pull-down are loaded in each lane. KLC was used as a negative control.

(legend continued on next page)

of peroxisomes around the centrosome was disrupted by overexpression of HA-p50/dynamitin and resulted in a random distribution of peroxisomes in both TRAK1-N-FRB and TRAK2-N-FRB-expressing cells (Figure 6J). Coexpression of myc-KIF5B redistributed the TRAK-N constructs to the cell periphery in ~70% of the cell (Figure 6J). These data demonstrate that the N-terminal domain in both TRAK1 and TRAK2 proteins is sufficient to induce microtubule plus-end and minus-end-directed transport. Interestingly, no significant differences were observed between TRAK1-N and TRAK2-N in these trafficking experiments, suggesting that additional mechanisms play a role in regulating the interaction between full-length TRAKs and kinesin-1.

TRAK2 Folds Back through a Head-to-Tail Interaction

To explain the distinct behaviors of TRAK1 and TRAK2, we further investigated the mechanism underlying the differential binding of TRAK1 and TRAK2 to kinesin-1. Some motor and adaptor proteins exist in a folded conformation, which allows the N-terminal and C-terminal regions to make direct contact and control their activity (Hirokawa and Noda, 2008). We explored whether such an intramolecular interaction occurs in TRAK proteins and could modulate the interaction with kinesin-1. We first tested whether the head and tail domains of TRAK can interact by coexpressed GFP-TRAK-N and myc-TRAK-C constructs in HEK293T cells and found that the two fragments coimmunoprecipitated with each other, in the case of both TRAK1 and TRAK2 (Figure 7A). More detailed mapping of the binding regions showed that the TRAK1-C interaction required the complete N-terminal domain (amino acids 1–360) of TRAK1 (Figures S6C and S6F), while further shortening of this region completely abolished binding of TRAK1-C (data not shown).

Next, we reasoned that attaching fluorophores to the NH2 and COOH termini of TRAK proteins (CFP donor and YFP acceptor) would allow us to detect fluorescence resonance energy transfer (FRET) if TRAK proteins indeed fold back and the NH2 and COOH termini come in close proximity. We generated TRAK1 and TRAK2 fusion constructs with YFP at the NH2 terminus and CFP at the COOH terminus (YFP-TRAK1-CFP and YFP-TRAK2-CFP) and used three different methods to determine the N- and C-terminal interacts, including FRET measurements in extracts, fluorescence lifetime imaging microscopy (FLIM), and acceptor photobleaching in single cells. First, HEK293T cells were transfected with plasmids, expressing CFP and YFP (negative control), CFP-YFP tandem fusion (positive control), YFP-TRAK1-CFP, or YFP-TRAK2-CFP, and the fluorescence spectra of the resulting cell extracts were measured (Lansbergen et al., 2004). Cell extracts containing both CFP and YFP displayed no significant emission of the YFP acceptor after the excitation of the CFP donor, while CFP-YFP displayed marked sensitized YFP fluorescence after CFP excitation due to FRET (Figure 7B, blue arrowhead). A marked YFP-sensitized emission was displayed by the YFP-TRAK2-CFP and less by the YFP-TRAK1-CFP-containing cell extract (Figure 7B, red and green arrowheads). The occurrence of FRET in the extract containing the YFP-TRAK2-CFP fusion is indicated by the ~20% higher ratio of fluorescence at 527 nm (YFP emission) to fluorescence at 475 nm (CFP emission) upon excitation at 425 nm, as compared with CFP + YFP mixture (Figure 7B). In contrast, YFP-TRAK1-CFP showed a small, nonsignificant fluorescent increase at 527 nm in this assay (Figure 7B). The ratio of YFP-to-CFP fluorescence in the extract, containing YFP-TRAK2-CFP protein, did not change after it was diluted, suggesting that the binding between the TRAK2 head and tail was intramolecular and not intermolecular (data not shown).

Next, we performed FRET measurements using FLIM in fixed (Figure 7D) and live COS7 cells (Figures 7C and 7E) expressing the constructs described above. FRET was detected by the decrease in CFP lifetime when YFP was in close proximity. As expected, cells expressing YFP-CFP tandem showed clear decrease in CFP lifetime compared to cells expressing CFP alone or with plasmid mixture of CFP+ YFP. Next, we determined FRET signals in cells expressing YFP-TRAK1-CFP or YFP-TRAK2-CFP and found that the TRAK2 construct showed a significantly higher FRET efficiency (Figure 7D). Similar data are obtained in live cells (Figures 7C and 7E). These results were confirmed by acceptor photobleaching approaches, where bleaching of YFP in YFP-CFP-positive FRET pairs dequenches CFP fluorescence and results in increased CFP fluorescence. With this method, only YFP-TRAK2-CFP showed a significant increase in CFP fluorescence intensity (Figure 7G). In all these experiments, TRAK2 consistently displays a significant FRET signal, suggesting an intramolecular association between the N- to C-terminal domains of the molecule. We believe that TRAK2 forms a relatively stabile head-to-tail interaction, while folding of full-length TRAK1 is more dynamic, short lived, and transient, suggesting that some properties of TRAK1 preclude its efficient self-folding.

Conformational Changes in TRAK Regulate KIF5 Binding and Mitochondrial Sorting

While TRAK2 did not associate with endogenous KIF5B, but overexpression of myc-KIF5B could force an interaction (Figure 5), we reasoned that the folded TRAK2 conformation might compete with endogenous kinesin-1 binding and that high concentrations of KIF5B might release the inhibitory state by unfolding TRAK2. Extracts prepared from cells cotransfected with myc-KIF5B and YFP-TRAK2-CFP, in the absence or presence of the TRAK-binding partner Miro (myc-Miro), no longer displayed a significant FRET signal, while YFP-sensitized

(C–E) Immunoprecipitations (IP) using GFP antibodies from extracts of HEK293 cells transfected with GFP-p150Glued and myc-TRAK1, myc-TRAK2 or myc-GRASP-1 (control) and probed for GFP or myc (C), GFP-TRAK1, GFP-TRAK2 or GFP (control) and probed for endogenous KIF5B, myc-Miro-1 and GFP (D), myc-KIF5B and indicated GFP-TRAK constructs and probed for myc or GFP (E).

(F) Biotin pull-downs (PD) from HEK293 extracts transfected with myc-TRAK1 or myc-TRAK2 and indicated biotin-tagged dynein/dynactin constructs and probed for GFP/HA and myc. The ratio input/pellet is 2%–5% for all pull-down and immunoprecipitation experiments.

(G) HeLa cells transfected with GFP-TRAK2 and stained with anti-p150Glued. Magnified areas show accumulation of p150Glued in the pericentrosomal region. Scale bar, 10 μm.

See also Figure S6 and Table S2.

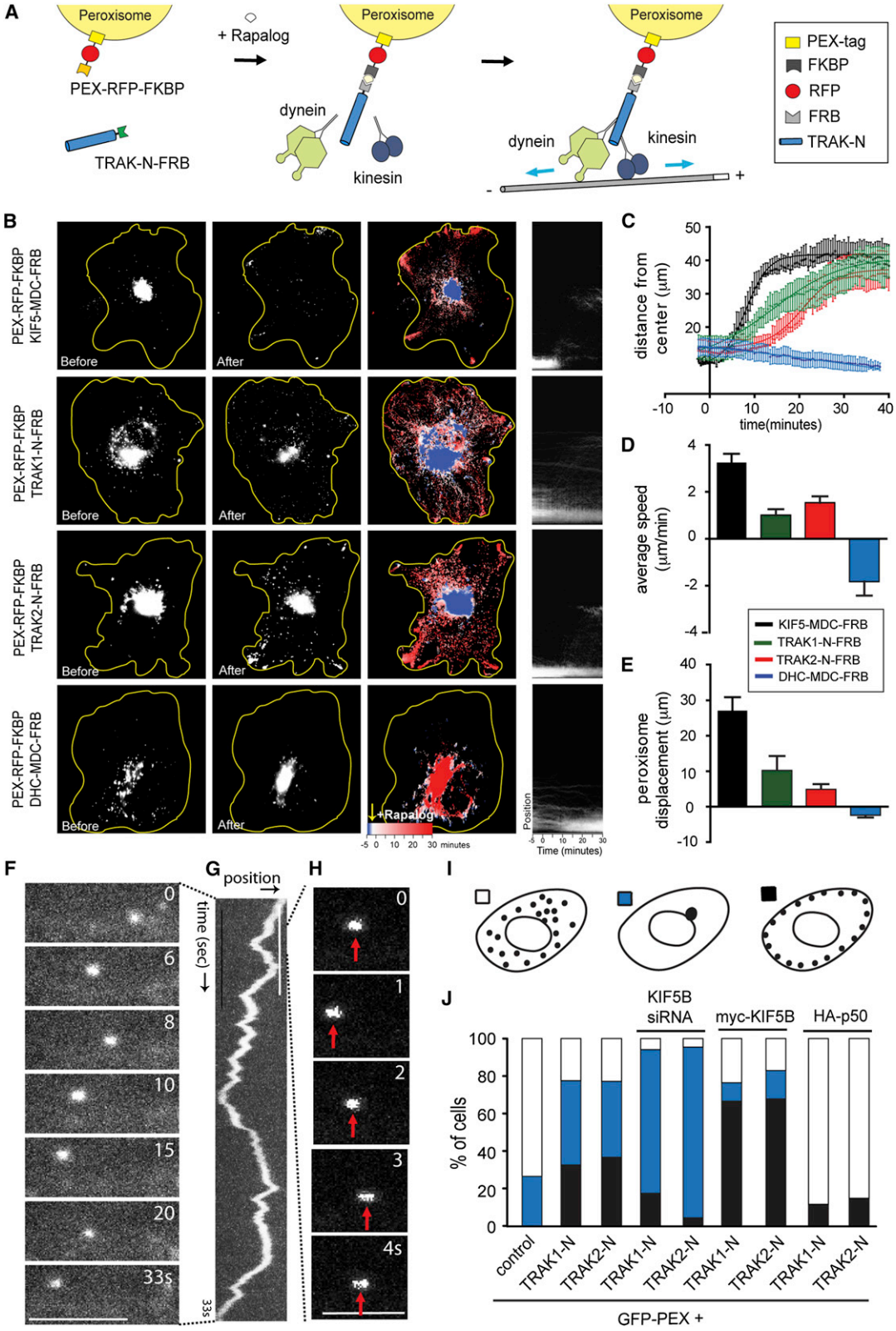

Figure 6. The TRAK N-Terminal Domain Mediates Bidirectional Motility

(A) Inducible cargo-trafficking assay. Fusions of FRB with truncated TRAK fragment (TRAK-N-FRB) are recruited to PEX-RFP-FKBP upon addition of rapalog.

(legend continued on next page)

emission was still detected in the extract of cells transfected with YFP-TRAK2-CFP alone, or YFP-TRAK2-CFP together with myc-Miro (Figure 7B; data not shown). Moreover, pull-down experiments comparing TRAK1-N only and TRAK1-N/TRAK1-C complexes indicate that a reduced amount of KIF5B is precipitated in the presence of TRAK1-C (Figure S6G), consistent with the idea that the intramolecular interaction in TRAK proteins and TRAK binding to KIF5B are mutually exclusive.

If the "open" TRAK conformation correlates with KIF5B binding, while the "closed" conformation inhibits it, forcing TRAK1 to fold back might make it more similar to TRAK2 and allow translocation from the axon to dendrites. To test this idea, we again used the rapamycin-mediated FRB-FKBP heterodimerization system but now fused the FRB and FKBP domains to the NH2 terminus and COOH terminus of TRAK1 and TRAK2 (FRB-HA-TRAK1-FKBP and FRB-HA-TRAK2-FKBP), respectively, causing a tight interaction between the C-terminal and N-terminal parts of TRAK after rapalog addition (Figure 8A). We first tested the system in HeLa cells by expressing FRB-HA-TRAK1-FKBP or FRB-HA-TRAK2-FKBP and treating cells with rapalog for different time periods (0, 15, and 30 min). Already 15 min after the addition of rapalog, the number of FRB-HA-TRAK1-FKBP cells with a pericentral TRAK1 localization shifted from ~10% (control 0 min rapalog) to ~60% (Figure 8C), suggesting a change in balance from plus-end-directed to minus-end-directed transport. No marked effect was observed in cell expressing FRB-HA-TRAK2-FKBP. Next, neurons were transfected with FRB-HA-TRAK1-FKBP or FRB-HA-TRAK2-FKBP constructs and treated with rapalog for different periods of time: 0, 30 min, and 2 hr. In control situation (0 min rapalog), the localization of TRAK1 and TRAK2 in axons and dendrites was similar to that described before. However, the addition of rapalog for 30 min caused a marked translocation of TRAK1 from the axonal compartment to the dendritic branches (Figure 8D), while TRAK2 maintained its dendritic distribution (data not shown). The change in PI reflects the strong enrichment of TRAK1 in dendrites (Figure 8E). The lack of KIF5B binding with the rapalog-induced "closed" conformation of FRB-HA-TRAK1-FKBP was confirmed by immunoprecipitation experiments, while the binding for dynein/dynactin was unaffected (Figure 8B). Together, these data strongly indicate that conformational differences between TRAK proteins control motor binding and regulate polarized mitochondrial sorting in neurons.

DISCUSSION

Complex processes critical for neuronal polarization have adapted basic cellular pathways to achieve the functional specialization of axons and dendrites. Some of these processes, such as cargo trafficking, require additional layers of control and significant fine-tuning. Here, we describe a molecular mechanism that efficiently coordinates mitochondrial transport in neurons. We demonstrate that the TRAK family proteins are bidirectional motor adaptors that differ in their function to transport mitochondria into axons and dendrites. TRAK1 binds to both kinesin-1 and dynein/dynactin, is prominently localized in axons, and is required for axonal outgrowth, whereas TRAK2 predominantly interacts with dynein/dynactin, is more abundantly present in dendrites, and is required for dendritic development. Moreover, we show that the differential function of the TRAK proteins can be explained by conformational differences. Our data suggest that TRAK2 adopts a folded conformation through an association between its NH2 and COOH termini, which inhibits the binding to kinesin-1 and prevents axonal transport.

Mammalian TRAK Proteins Control Mitochondria Trafficking in Polarized Cells

Previous work examining the role of motor proteins in axonal mitochondrial transport revealed that the opposite-polarity motors kinesin-1 and dynein drive anterograde and retrograde transport, respectively (Boldogh and Pon, 2007; Frederick and Shaw, 2007; Saxton and Hollenbeck, 2012). In many models, targeting of mitochondria depends on kinesin-1's ability to overcome the opposing effect of dynein, and understanding motor protein regulation has become a key challenge to interpret retrograde versus anterograde motility. It is clear that the activity of both opposite-polarity motors triggers bidirectional transport, which is most likely regulated by cargo-adaptor proteins (Welte, 2004). Here, we show that kinesin-1 and dynein/dynactin cooperate to control trafficking of mitochondria in the axon. Inhibition of kinesin-1 or dynein alone reduced motility in both retrograde and anterograde directions, consistent with detailed genetic analysis of mitochondrial movement in *Drosophila* larval motor axons (Pilling et al., 2006). This is in agreement with other model systems where kinesin-1 and cytoplasmic dynein require each other for bidirectional transport of intracellular cargo (Ally et al., 2009). In contrast, we show that mitochondria motility in dendrites only requires dynein motor activity, which is consistent

(B) Peroxisome distribution before and after rapalog addition in the presence of TRAK1-N-FRB, TRAK2-N-FRB, the truncated motor construct of kinesin-1 (KIF5-MDC-FRB) or DHC (DHC-MDC-FRB). Yellow lines indicate COS7 cell outline. The overlay of sequential binarized images is color coded by time. Radial kymographs for the recordings are indicated in right panel.
(C) Time traces of $R_{90\%}$ for cells transfected with the KIF5-MDC-FRB (n = 9; black line), TRAK1-N-FRB (n = 5; green line), TRAK2-N-FRB (n = 9; red line), and DHC-MDC-FRB (n = 8; blue line). Sigmoid curves were fitted. Note that $R_{90\%}$ is the radius for each time point that includes 90% of the total fluorescent intensity.
(D) Graph shows the average speed of peroxisomes as calculated from time traces of $R_{90\%}$.
(E) Graph shows peroxisome displacement 15 min after addition of rapalog.
(F–H) Time series shows translocation of TRAK2-N-FRB-mediated cargo after addition of rapalog within 33 s (F) and 5 s (H). Scale bars, 5 μm. The recordings in (F) and (H) are shown in a kymograph (G). Bidirectional motion is observed after TRAK2-N recruitment to the peroxisome.
(I) Schematic overview of the three distribution patterns observed in HeLa cells using the peroxisome-based trafficking assay; random distribution (white), peripheral (black), or pericentral (blue) accumulations.
(J) Percentage of HeLa cells shows dispersed, pericentrosomal, or peripheral distribution of PEX-GFP alone compared to double transfection with TRAK1-N, or TRAK2-N and triple transfection with KIF5B siRNA, myc-KIF5B, or HA-p50 constructs.
See also Movie S8.

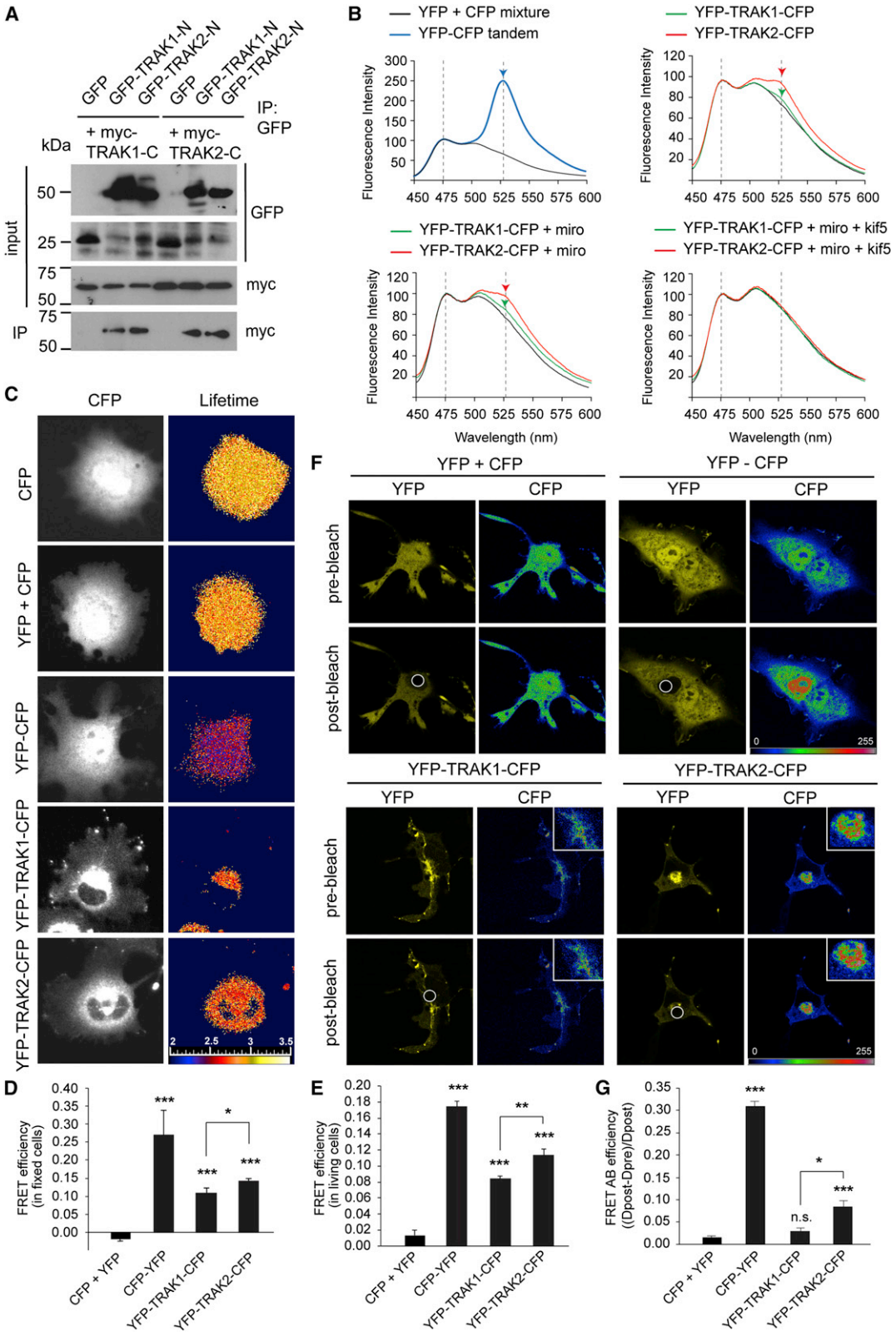

Figure 7. Intramolecular Head-to-Tail Interactions in TRAK2 Measured by FRET in Living Cells

(A) Coimmunoprecipitations from extracts of HEK293 cells cotransfected with indicated constructs.

(legend continued on next page)

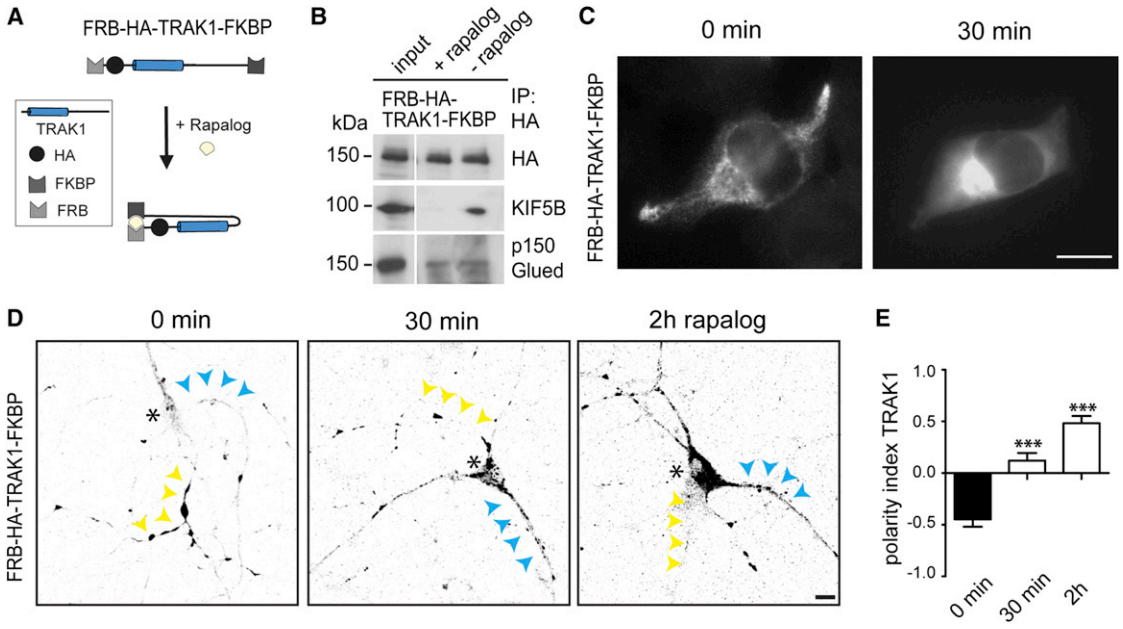

Figure 8. Conformational Changes in TRAK Proteins Regulate Mitochondrial Sorting

(A) Schematic overview of FRB-rapalog-FKBP system used to induce folding of TRAK proteins.

(B) Immunoprecipitations using HA antibodies from extracts of HeLa cells transfected with FRB-HA-TRAK1-FKBP and treated with (+) or without (−) rapalog for 10 min.

(C) Representative images of transfected HeLa cells with FRB-HA-TRAK1-FKBP before (0 min) and after (30 min) addition of rapalog. The number of cells with a pericentral TRAK1 localization shifted from ~10% to ~60% within this time frame ($p < 0.05$; n = 3 independent experiment). Scale bar, 10 μm.

(D) Representative images of hippocampal neurons at DIV 12+2 transfected with FRB-HA-TRAK1-FKBP before (0 min) and after (30 min and 2 hr) addition of rapalog. Scale bar, 10 μm.

(E) PI of FRB-HA-TRAK1-FKBP in hippocampal neurons at DIV 12+2 before (0 min) and after (30 min and 2 hr) addition of rapalog. Three independent experiments (n > 15 neurons) were performed. Error bars indicate SEM. ***$p < 0.001$.

with dynein-only-coupled cargos moving in a bidirectional fashion along antiparallel dendritic microtubules (Kapitein et al., 2010b).

Recent work has also revealed that, in addition to bidirectional transport, kinesin-1 and dynein/dynactin proteins play important roles in selective trafficking into axons and dendrites (Kapitein and Hoogenraad, 2011). Studies in both *Drosophila* and mammalian neurons indicated that kinesin-1 motors, often in concert with dynein (Kwinter et al., 2009; Pilling et al., 2006), drive transport into the axon, while the dynein/dynactin complex is the key motor for selective transport into dendrites (Kapitein et al., 2010a; Zheng et al., 2008). The axonal targeting of kinesin-1 is governed by microtubule modifications that enhance kinesin-1 binding, whereas dynein-dependent cargo sorting to dendrites is facilitated by the minus-end distal-oriented microtubules exclusively present in dendrites (Kapitein et al., 2010a; Rolls, 2011). Our data demonstrate that kinesin-1 motors drive mitochondria transport into axons and require dynein/dynactin for their activity, while dynein/dynactin steers mitochondria trafficking into dendrites independently of kinesin-1. The strong and opposite targeting preferences of these mitochondrial transport motors in axons and dendrites suggest that establishing nonpolarized transport of mitochondria requires fine-tuning of dynein and kinesin-1 motor protein activity. Our data suggest that mammalian TRAK1 and TRAK2 differentially employ these two transport machineries and together mediate selective mitochondrial trafficking in polarized cells. We propose a model in which kinesin-1 drives mitochondria transport into axons and requires

(B) Emission spectrums of the extracts prepared from HEK293 cells transfected with TRAK1 (green line) or TRAK2 (red line) constructs fused to YFP and CFP or corresponding controls (including YFP + CFP [black line] and YFP-CFP tandem [blue line]), measured with excitation at 425 nm. Fluorescence intensity is shown in arbitrary units.

(C) COS7 cells were transfected with indicated constructs. The lifetime of CFP was measured and compared to YFP + CFP as negative control and YFP-CFP tandem FRET construct as positive control. The lifetimes are presented in pseudocolor scale (2–3.5 ns range).

(D and E) Statistical analysis of FRET efficiency for fixed (D) and living (E) COS7 cells transfected with the constructs represented in (C). Between 6 and 12 cells were measured per group. Error bars indicate SEM. *$p < 0.05$; **$p < 0.01$; ***$p < 0.001$.

(F) Acceptor bleaching FRET of indicated constructs in COS7 cells. Pre- and postbleached images of YFP and CFP channels are depicted. Bleached area of the acceptor (YFP) is indicated in white circle. CFP intensity images are presented in pseudocolor scale (0–255).

(G) Quantification of FRET acceptor bleaching (AB) efficiency. CFP intensities in the bleached area were measured before and after bleaching of YFP and plotted as mean FRET AB efficiency. Between 10 and 31 cells were measured per group. Error bars indicate SEM. *$p < 0.05$; **$p < 0.01$. n.s., not significant.

dynein for its activity (controlled by TRAK1), and dynein steers mitochondria trafficking into dendrites independently of kinesin-1 (controlled by TRAK2).

Several lines of evidence support this model. First, we show that TRAK1 and TRAK2 have a polarized distribution in hippocampal neurons. TRAK1 is prominently localized in axons, while TRAK2 is more abundantly present in dendrites. Second, increased TRAK1 expression levels drive mitochondria in the axon, while overexpression of TRAK2 leads to the accumulation of mitochondria in dendrites. These opposing effects were also observed in nonneuronal cells, where TRAK1 expression exhibits a more peripheral localization, and TRAK2 shows a central localization. Third, TRAK1 and TRAK2 associate with different motor protein complexes: TRAK1 binds to both kinesin-1 and dynein/dynactin, while TRAK2 predominantly interacts with dynein/dynactin. This suggests that TRAK2 is predominately linked to minus-end-directed transport motors, which makes it an ideal candidate for targeting mitochondria to dendrites. We propose that TRAK2 controls transport of mitochondria from the cell body into dendrites by promoting dynein binding. Consistently, our data show that dynein/dynactin is required for the proper dendritic distribution of mitochondria and that direct coupling of dynein to mitochondria drives their transport into dendrites. Once mitochondria are inside axons or dendrites, the final targeting, such as to synapses, could be achieved through selective retention at target sites (Kang et al., 2008) or specific delivery by additional actin-dependent motors such as myosin V (Saxton and Hollenbeck, 2012).

Conformational Differences between TRAK Proteins Govern Mitochondrial Trafficking

Our data support the motor-adaptor model for *Drosophila* Milton that proposes that linkage of mitochondria to the transport machinery involves Milton/TRAK adaptors that bind to microtubule-based motors (Boldogh and Pon, 2007; Goldstein et al., 2008; MacAskill and Kittler, 2010). Expression of Milton in HEK293 cells also showed clustering of mitochondria near the microtubule-organizing center (Stowers et al., 2002), suggesting that *Drosophila* Milton might interact with components of the dynein/dynactin complex. Moreover, several Milton splice variants have been described in flies that differentially bind to kinesin-1 (Glater et al., 2006). The splice variant Milton-C shows remarkable similarities with TRAK2: it induces pericentrosomal accumulation of mitochondria and binds relatively poorly to kinesin-1 (Glater et al., 2006).

To explain the functional differences between TRAK1 and TRAK2, we propose that TRAK2 proteins change their protein conformation as a result of interaction of the N-terminal coiled-coil region and C-terminal domain, thereby affecting the interaction with KIF5B. Our data demonstrate that the intramolecular TRAK2 interaction and KIF5B binding are mutually exclusive. Thus, only when the N-terminal TRAK2 domain detaches from the C-terminal tail domain does this N-terminal region become available for kinesin-1 binding. The binding of TRAK2 to the mitochondrial adaptor Miro and to components of the dynein/dynactin complex is not dependent on TRAK protein folding. Therefore, TRAK2-enriched mitochondria will predominantly contain dynein/dynactin and subsequently drive mitochondria into the dendrites. In contrast, TRAK1 is largely precluded from efficient self-folding, interacts with KIF5, and drives mitochondria into axons. Induced folding of TRAK1 by using the FRB-rapalog-FKBP system makes it behave similar to TRAK2 and promotes its translocation from the axon to dendrites. Consistent with the data that folded TRAK conformations compete with kinesin-1 binding, the rapalog-induced "closed" TRAK1 does not longer bind to KIF5B, while the interaction with dynein/dynactin is unaffected.

Mitochondria in axon and dendrite have both TRAK proteins and opposing motors on them in both compartments. This implies that concentration differences of TRAK1 and TRAK2 on mitochondria can balance the transport in either the anterograde or retrograde direction and subsequently steers mitochondria trafficking to axons or dendrites. Mitochondria with higher TRAK2 levels have a higher chance to be transported by dynein, while mitochondria on which TRAK1 is more abundant are more frequently transported by kinesin-1. This differential transport also explains why more TRAK1 accumulates in axons and more TRAK2 in dendrites; the polarized TRAK pools can further promote differential transport of mitochondria within the two neuronal compartments. However, this is probably not the complete picture. TRAK1 and TRAK2 can most likely, at least partly, compensate for each other's function. For example, TRAK1 can form an N- and C-terminal interaction and show FRET signals in single-cell assays, and TRAK1 knockdown reveals a mild dendrite morphology phenotype with some trafficking defects. Moreover, knockdown of TRAK1/TRAK2 and inhibition of dynein/dynactin and kinesin-1 do not completely stop mitochondrial motility but inhibit axonal and dendritic transport about 2- to 3-fold. Therefore, it is expected that additional motor proteins but also coordinating factors and signaling proteins will participate in regulating bidirectional movements and polarized mitochondria transport in neurons. Recent work characterized Miro's role as a calcium sensor for the regulation of mitochondrial dynamics and bidirectional transport (Macaskill et al., 2009; Russo et al., 2009; Wang and Schwarz, 2009) and found a role for O-GlcNAc OGT (Brickley et al., 2011; Iyer et al., 2003) and PINK1 (Liu et al., 2012; Wang et al., 2011) in controlling mitochondrial dynamics. Moreover, it is tempting to speculate that conformational switching of TRAK proteins is an additional mechanism for local motor protein regulation. Additional studies are required to determine whether other adaptor/motor complexes participate in mitochondria transport and whether local signaling can influence polarized trafficking.

In this study, we established a key role for mammalian TRAK proteins in axonal and dendritic targeting of mitochondria. We found that TRAK proteins are important for uniform mitochondria distribution in polarized cells and both axon and dendritic morphology. Expression of individual TRAK proteins changes the distribution of mitochondria in axons or dendrites. Alterations in mitochondrial transport have been described in kinesin and dynein mutant mice (Tanaka et al., 1998; Wiggins et al., 2012) and are correlated with several neurodegenerative diseases (Chan, 2006; Mattson et al., 2008). Our current findings provide molecular targets to investigate the axonal and dendritic mitochondrial transport machinery in neurodegenerative disease models. Future studies using genetic disease mouse models

will help to elucidate the mechanisms regulating the molecular interplay between motors, bidirectional adaptor and polarized transport machinery and advance our understanding of neurodegenerative disorders.

EXPERIMENTAL PROCEDURES

Antibodies and Reagents

cDNAs encoding human TRAK1 (amino acids 754–953) and TRAK2 (amino acids 848–913) were cloned into pGEX-4T to generate glutathione S-transferase (GST) fusion proteins. Rabbit anti-TRAK1 and anti-TRAK2 antibodies were generated by immunizing rabbits with GST-TRAK fusion proteins. Details of TRAK antisera and other antibodies and reagents are in the Supplemental Experimental Procedures.

DNA Constructs

The TRAK1 and TRAK2 expression constructs and their deletion mutants were generated by a PCR-based strategy using the human TRAK1 cDNA (KIAA1042, a gift from Kazusa DNA Research Institute) and human TRAK2 cDNA (IMAGE clone 4814594). The TRAK1#1 (5′-GCTGTCGCAAATCGTGGACTT-3′), TRAK1#2 (5′-GTGTACTGCCTTAACGACT-3′), TRAK2#1 (5′-GCTTGTCACATCAAGACAGAA-3′), and TRAK2#2 (5′-CGCTACATGATTCTAGGCA-3′) sequences targeting rat TRAK1 mRNA (NM_001042646.1) and TRAK2 mRNA (NM_015049.1) were designed by using the siRNA selection program at the Whitehead Institute for Biomedical Research. For details, see Supplemental Experimental Procedures.

Primary Hippocampal Neuron Cultures and Transfection

Primary hippocampal cultures were prepared from embryonic day 18 (E18) rat brains and transfected using Lipofectamine 2000 (Invitrogen).

Image Acquisition, Processing, and Morphometric Analyses

Simultaneous dual-color time-lapse live-cell imaging and TIRFM were performed on a Nikon Eclipse TE2000E microscope with CoolSNAP and QuantEM cameras (Roper Scientific). Neurons were maintained at 37°C with 5% CO_2 (Tokai Hit). FRET-FLIM measurements on fixed and living cells expressing YFP and CFP fused to the NH2 and COOH terminus of TRAKs and corresponding controls were performed on a PCM-2000 Confocal microscope equipped with a time-gated fluorescence lifetime imaging module (LiMo; Nikon Instruments). FRET acceptor photobleaching experiments were performed on SP5 CLSM systems (Leica-Microsystems). For details, see Supplemental Experimental Procedures.

SUPPLEMENTAL INFORMATION

Supplemental Information includes six figures, two tables, eight movies, and Supplemental Experimental Procedures and can be found with this article online at http://dx.doi.org/10.1016/j.neuron.2012.11.027.

ACKNOWLEDGMENTS

We thank Dr. David Stephens for GFP-p150Glued, Dr. Richard Vallee for Flag-DHC-FL, Dr. Pontus Aspenström for myc-Miro-1, Karel Bezstarosti for help with mass spectrometry analyses, and Dr. Esther de Graaff for TRAK antibody-blocking experiments. J.L. is supported by International PhD Projects Programme of Foundation for Polish Science (studies of nucleic acids and proteins-from basic to applied research) cofinanced by the European Union-Regional Development Fund and cosupervised by Dr. Jacek Jaworski. M.M. is a recipient of a European Molecular Biology Organization (EMBO) Long-Term Fellowship (EMBO ALTF 884-2011) cofunded by the European Commission (EMBOCOFUND2010, GA-2010-267146) and Marie Curie Actions. This work was supported by the Erasmus Medical Center (EMC fellowship to L.C.K.), the Netherlands Organisation for Scientific Research (NWO-VENI to L.C.K. and NWO-ALW-VICI to A.A. and C.C.H.), the Netherlands Organisation for Health Research and Development (ZonMW-TOP to C.C.H.), the European Science Foundation (EURYI to C.C.H.), EMBO Young Investigators Program (to C.C.H.), and the Human Frontier Science Program (HFSP-CDA to C.C.H.).

Accepted: November 8, 2012
Published: February 6, 2013

REFERENCES

Ally, S., Larson, A.G., Barlan, K., Rice, S.E., and Gelfand, V.I. (2009). Opposite-polarity motors activate one another to trigger cargo transport in live cells. J. Cell Biol. *187*, 1071–1082.

Boldogh, I.R., and Pon, L.A. (2007). Mitochondria on the move. Trends Cell Biol. *17*, 502–510.

Brickley, K., and Stephenson, F.A. (2011). Trafficking kinesin protein (TRAK)-mediated transport of mitochondria in axons of hippocampal neurons. J. Biol. Chem. *286*, 18079–18092.

Brickley, K., Smith, M.J., Beck, M., and Stephenson, F.A. (2005). GRIF-1 and OIP106, members of a novel gene family of coiled-coil domain proteins: association in vivo and in vitro with kinesin. J. Biol. Chem. *280*, 14723–14732.

Brickley, K., Pozo, K., and Stephenson, F.A. (2011). N-acetylglucosamine transferase is an integral component of a kinesin-directed mitochondrial trafficking complex. Biochim. Biophys. Acta *1813*, 269–281.

Chan, D.C. (2006). Mitochondria: dynamic organelles in disease, aging, and development. Cell *125*, 1241–1252.

Frederick, R.L., and Shaw, J.M. (2007). Moving mitochondria: establishing distribution of an essential organelle. Traffic *8*, 1668–1675.

Glater, E.E., Megeath, L.J., Stowers, R.S., and Schwarz, T.L. (2006). Axonal transport of mitochondria requires milton to recruit kinesin heavy chain and is light chain independent. J. Cell Biol. *173*, 545–557.

Goldstein, A.Y., Wang, X., and Schwarz, T.L. (2008). Axonal transport and the delivery of pre-synaptic components. Curr. Opin. Neurobiol. *18*, 495–503.

Guo, X., Macleod, G.T., Wellington, A., Hu, F., Panchumarthi, S., Schoenfield, M., Marin, L., Charlton, M.P., Atwood, H.L., and Zinsmaier, K.E. (2005). The GTPase dMiro is required for axonal transport of mitochondria to *Drosophila* synapses. Neuron *47*, 379–393.

Hirokawa, N., and Noda, Y. (2008). Intracellular transport and kinesin superfamily proteins, KIFs: structure, function, and dynamics. Physiol. Rev. *88*, 1089–1118.

Hoogenraad, C.C., Wulf, P., Schiefermeier, N., Stepanova, T., Galjart, N., Small, J.V., Grosveld, F., de Zeeuw, C.I., and Akhmanova, A. (2003). Bicaudal D induces selective dynein-mediated microtubule minus end-directed transport. EMBO J. *22*, 6004–6015.

Iyer, S.P., Akimoto, Y., and Hart, G.W. (2003). Identification and cloning of a novel family of coiled-coil domain proteins that interact with O-GlcNAc transferase. J. Biol. Chem. *278*, 5399–5409.

Kang, J.S., Tian, J.H., Pan, P.Y., Zald, P., Li, C., Deng, C., and Sheng, Z.H. (2008). Docking of axonal mitochondria by syntaphilin controls their mobility and affects short-term facilitation. Cell *132*, 137–148.

Kapitein, L.C., and Hoogenraad, C.C. (2011). Which way to go? Cytoskeletal organization and polarized transport in neurons. Mol. Cell. Neurosci. *46*, 9–20.

Kapitein, L.C., Schlager, M.A., Kuijpers, M., Wulf, P.S., van Spronsen, M., MacKintosh, F.C., and Hoogenraad, C.C. (2010a). Mixed microtubules steer dynein-driven cargo transport into dendrites. Curr. Biol. *20*, 290–299.

Kapitein, L.C., Schlager, M.A., van der Zwan, W.A., Wulf, P.S., Keijzer, N., and Hoogenraad, C.C. (2010b). Probing intracellular motor protein activity using an inducible cargo trafficking assay. Biophys. J. *99*, 2143–2152.

Kwinter, D.M., Lo, K., Mafi, P., and Silverman, M.A. (2009). Dynactin regulates bidirectional transport of dense-core vesicles in the axon and dendrites of cultured hippocampal neurons. Neuroscience *162*, 1001–1010.

Lansbergen, G., Komarova, Y., Modesti, M., Wyman, C., Hoogenraad, C.C., Goodson, H.V., Lemaitre, R.P., Drechsel, D.N., van Munster, E., Gadella, T.W., Jr., et al. (2004). Conformational changes in CLIP-170 regulate its binding to microtubules and dynactin localization. J. Cell Biol. *166*, 1003–1014.

Liu, S., Sawada, T., Lee, S., Yu, W., Silverio, G., Alapatt, P., Millan, I., Shen, A., Saxton, W., Kanao, T., et al. (2012). Parkinson's disease-associated kinase PINK1 regulates Miro protein level and axonal transport of mitochondria. PLoS Genet. *8*, e1002537.

MacAskill, A.F., and Kittler, J.T. (2010). Control of mitochondrial transport and localization in neurons. Trends Cell Biol. *20*, 102–112.

Macaskill, A.F., Rinholm, J.E., Twelvetrees, A.E., Arancibia-Carcamo, I.L., Muir, J., Fransson, A., Aspenstrom, P., Attwell, D., and Kittler, J.T. (2009). Miro1 is a calcium sensor for glutamate receptor-dependent localization of mitochondria at synapses. Neuron *61*, 541–555.

Mattson, M.P., Gleichmann, M., and Cheng, A. (2008). Mitochondria in neuroplasticity and neurological disorders. Neuron *60*, 748–766.

Pilling, A.D., Horiuchi, D., Lively, C.M., and Saxton, W.M. (2006). Kinesin-1 and Dynein are the primary motors for fast transport of mitochondria in *Drosophila* motor axons. Mol. Biol. Cell *17*, 2057–2068.

Rolls, M.M. (2011). Neuronal polarity in *Drosophila*: sorting out axons and dendrites. Dev. Neurobiol. *71*, 419–429.

Russo, G.J., Louie, K., Wellington, A., Macleod, G.T., Hu, F., Panchumarthi, S., and Zinsmaier, K.E. (2009). *Drosophila* Miro is required for both anterograde and retrograde axonal mitochondrial transport. J. Neurosci. *29*, 5443–5455.

Saxton, W.M., and Hollenbeck, P.J. (2012). The axonal transport of mitochondria. J. Cell Sci. *125*, 2095–2104.

Stowers, R.S., Megeath, L.J., Górska-Andrzejak, J., Meinertzhagen, I.A., and Schwarz, T.L. (2002). Axonal transport of mitochondria to synapses depends on milton, a novel *Drosophila* protein. Neuron *36*, 1063–1077.

Tanaka, Y., Kanai, Y., Okada, Y., Nonaka, S., Takeda, S., Harada, A., and Hirokawa, N. (1998). Targeted disruption of mouse conventional kinesin heavy chain, kif5B, results in abnormal perinuclear clustering of mitochondria. Cell *93*, 1147–1158.

Vale, R.D. (2003). The molecular motor toolbox for intracellular transport. Cell *112*, 467–480.

Wang, X., and Schwarz, T.L. (2009). The mechanism of Ca2+ -dependent regulation of kinesin-mediated mitochondrial motility. Cell *136*, 163–174.

Wang, X.N., Winter, D., Ashrafi, G., Schlehe, J., Wong, Y.L., Selkoe, D., Rice, S., Steen, J., LaVoie, M.J., and Schwarz, T.L. (2011). PINK1 and Parkin target Miro for phosphorylation and degradation to arrest mitochondrial motility. Cell *147*, 893–906.

Welte, M.A. (2004). Bidirectional transport along microtubules. Curr. Biol. *14*, R525–R537.

Wiggins, L.M., Kuta, A., Stevens, J.C., Fisher, E.M., and von Bartheld, C.S. (2012). A novel phenotype for the dynein heavy chain mutation Loa: altered dendritic morphology, organelle density, and reduced numbers of trigeminal motoneurons. J. Comp. Neurol. *520*, 2757–2773.

Zheng, Y., Wildonger, J., Ye, B., Zhang, Y., Kita, A., Younger, S.H., Zimmerman, S., Jan, L.Y., and Jan, Y.N. (2008). Dynein is required for polarized dendritic transport and uniform microtubule orientation in axons. Nat. Cell Biol. *10*, 1172–1180.